Macromolecules

Article

pubs.acs.org/Macromolecules

Single-Material Organic Solar Cells Based on Electrospun Fullerene-Grafted Polythiophene Nanofibers

Filippo Pierini,*[,†] Massimiliano Lanzi,[§] Paweł Nakielski,[†] Sylwia Pawłowska,[†] Olga Urbanek,[‡] Krzysztof Zembrzycki,[†] and Tomasz Aleksander Kowalewski[†]

[†]Department of Biosystems and Soft Matter, Institute of Fundamental Technological Research, and [‡]Laboratory of Polymers and Biomaterials, Institute of Fundamental Technological Research, Polish Academy of Sciences, Warsaw 02-106, Poland

[§]Department of Industrial Chemistry "Toso Montanari", Alma Mater Studiorum University of Bologna, Bologna 40136, Italy

Supporting Information

ABSTRACT: Highly efficient single-material organic solar cells (SMOCs) based on fullerene-grafted polythiophenes were fabricated by incorporating electrospun one-dimensional (1D) nanostructures obtained from polymer chain stretching. Poly(3-alkylthiophene) chains were chemically tailored in order to reduce the side effects of charge recombination which severely affected SMOC photovoltaic performance. This enabled us to synthesize a donor−acceptor conjugated copolymer with high solubility, molecular weight, regioregularity, and fullerene content. We investigated the correlations among the active layer hierarchical structure given by the inclusion of electrospun nanofibers and the solar cell photovoltaic properties. The results indicated that SMOC efficiency can be strongly increased by optimizing the supramolecular and nanoscale structure of the active layer, while achieving the highest reported efficiency value (PCE = 5.58%). The enhanced performance may be attributed to well-packed and properly oriented polymer chains. Overall, our work demonstrates that the active material structure optimization obtained by including electrospun nanofibers plays a pivotal role in the development of efficient SMOCs and suggests an interesting perspective for the improvement of copolymer-based photovoltaic device performance using an alternative pathway.

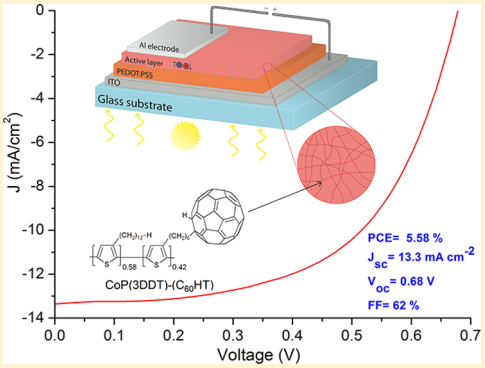

INTRODUCTION

Organic solar cells (OSCs) have received much attention due to their potential application in the development of flexible, lightweight, and cost-effective photovoltaic devices.[1] Bulk heterojunction (BHJ) cells are the most widely investigated OSCs.[2] Advances in their development have already made it possible to overcome the power conversion efficiency (PCE) threshold which is deemed necessary to make organic photovoltaics commercially attractive.[3] Despite these achievements, BHJ cells are still not widely produced commercially. Several additional parameters, other than PCE, affect the final applicability of BHJ devices.[4] BHJ cells are based on the blend of an electron donor and an electron acceptor. Since the active material should have a bicontinual and homogeneous nanoscale phase separation, the morphological optimization of this thermodynamically unstable blend is complicated and expensive.[5] This problem is intrinsic in the concept of BHJ and cannot be completely overcome. Nevertheless, not many scientific efforts are oriented toward other types of OSCs that can offer a compelling way to increase their applicability.

The covalent linking of electron accepting moieties (e.g., fullerenes) to a hole-transporting conjugated polymer as polythiophene, allowing intramolecular electron transfer from donors to acceptors, is the most elegant approach for overcoming the limitations of BHJ devices.[6] Since the active material is based on one component, the phase separation-related problem is solved. However, so far, single-material organic solar cell (SMOC) efficiency is severely affected by the charge recombination and ineffective transport.[7] The tailoring of the content, mode of linkage, position, and orientation of fullerenes into the conjugated polymer backbone has already limited the negative impact of charge recombination.[8] In spite of these advancements, SMOCs efficiency is lower than conventional BHJ cells' PCE, and the former are still uncompetitive devices. However, the experts in the field agree that focusing on molecular improvements while, at the same time, optimizing the charge transport is the best approach toward reaching a satisfying PCE.[1,2,5−7] Structure optimization of the active material is considered the key parameter for overcoming the limits of the previously developed OSCs.[9]

SMOC active layers are considered three-dimensional (3D) structures made of randomly oriented macromolecular units, where charges can move without following the ideal linear path.[7] Even though the development of efficient transport channels promoting the formation of optimal percolation paths for the charges is crucial for increasing the SMOC efficiency,

Received: April 25, 2017
Revised: June 16, 2017
Published: June 28, 2017

DOI: 10.1021/acs.macromol.7b00857
Macromolecules 2017, 50, 4972−4981

this aspect is still unexplored. Some recent studies, however, show that electrospinning is the most efficient technique for elongating and aligning polymer chains to form nanofibers with a well-defined hierarchical structure.[10−12]

Here we report on the synthesis of a new donor−acceptor conjugated copolymer poly[3-dodecylthiophene-*co*-3-(6-fullerenylhexyl)thiophene] (CoP(3DDT)-(C_{60}HT)), with high regioregularity, molecular weight, fullerene content, and solubility. We then produced continuous, uniform electrospun nanofibers. The CoP(3DDT)-(C_{60}HT) 1D nanomaterials were integrated into SMOCs, and last, the supramolecular structuration was improved by thermal annealing.

We investigated the contribution of intramolecular heterojunction design, supramolecular structure optimization, and nanostructured architecture assessment with a comparative study. Our cell already proved to perform better than conventional BHJ solar cells and showed that its PCE is consistently higher than the most efficient SMOC developed up to now. For the first time, we demonstrated an efficient SMOC with a PCE greater than 5.5% achieved by tailoring the active layer hierarchical structure.

EXPERIMENTAL SECTION

Synthesis and Characterization of CoP(3DDT)-(C_{60}HT). All reagents were commercially available and were used as received without further purification unless otherwise stated. To a solution of 2.51 g (6.13 mmol) of 2,5-dibromo-3-dodecylthiophene and 2.48 g (6.13 mmol) of 2,5-dibromo-3-(6-bromohexyl)thiophene, prepared according to the Lanzi et al. method,[13] in 100 mL of anhydrous THF, 4.09 mL (12.26 mmol) of a 3 M solution of methylmagnesium chloride in THF was added. The reaction mixture was refluxed for 2 h under stirring and a gentle flux of nitrogen. Afterward, 33.2 mg (0.062 mmol) of [1,3-bis(diphenylphosphino)propane]nickel(II) chloride was added, and the mixture was refluxed again for 1 h. After cooling to room temperature, the mixture was dropped into 650 mL of methanol, and the precipitate was filtered through a PTFE membrane (0.45 μm pore size). The recovered polymer was washed several times with methanol and dried, giving 2.22 g (8.95 mmol) of poly[3-dodecylthiophene-*co*-3-(6-bromohexyl)thiophene] (73% yield).

To 0.062 mg (2.56 mmol) of Mg turnings, 0.559 g (2.25 mmol) of poly[3-dodecylthiophene-*co*-3-(6-bromohexyl)thiophene] was added, under stirring and in an inert atmosphere. The reaction mixture was refluxed for 5 h, cooled down to room temperature, and transferred via cannula to a solution of 0.540 g (0.748 mmol) of C_{60}-fullerene in 150 mL of anhydrous toluene and 1.50 mL of anhydrous *N*,*N*-dimethylformamide. The mixture was reacted at 25 °C for 30 min under stirring in an inert atmosphere. The reaction was then quenched with a solution of 50 mg of ammonium chloride in 5 mL of distilled water and subsequently added to 150 mL of brine. The organic layer was washed with distilled water to neutrality, dried with magnesium sulfate, and concentrated. The copolymer was then fractionated using a toluene/*n*-heptane (1:3 v/v) mixture. After filtration through a PTFE membrane (0.20 μm pore size), 0.989 g of fractionated CoP(3DDT)-(C_{60}HT) was obtained (85% yield).

The ^{1}H NMR spectra were recorded on a Varian Mercury Plus 400 (400 MHz, room temperature) spectrometer using tetramethylsilane (TMS) as internal reference. Fourier transform infrared (FT-IR) spectra were taken on Ge disks using a PerkinElmer Spectrum One spectrophotometer. Molecular weight and polydispersity of the polymer were determined with gel permeation chromatography (GPC) using polystyrene standards and THF as an eluent on a HPLC Lab Flow 2000 apparatus equipped with a Phenomenex Phenogel 5 μ MXL mixed bed column and a Linear Instrument UV−vis detector model UVis 200 working at 263 nm.

Electrospinning of CoP(3DDT)-(C_{60}HT) Nanofibers. First, the precursor solutions were prepared by dissolving 66 mg of CoP-(3DDT)-(C_{60}HT) in 1.3 mL of chloroform and 40 mg of poly(ethylene oxide) (PEO) in 2 mL of chloroform, separately, with stirring at 50 °C for 48 h. 0.7 mL of PEO solution was successively added to the CoP(3DDT)-(C_{60}HT) solution in order to prepare the electrospinning mixture containing 3.3 wt % of CoP(3DDT)-(C_{60}HT) and 0.7 wt % of PEO in chloroform. A uniform reddish-brown viscous solution was obtained after stirring for 24 h. The polymer solution was loaded into a syringe fitted with a metal needle with an inner diameter of 0.4 mm. Subsequently, the solution was electrospun at a constant flow rate of 0.45 mL h^{-1} using a syringe pump (KD Scientific syringe pump model 200-CE) and at a high voltage (8.5 kV) generated by a high-voltage power supply (Spellman model SL150) connected to the needle. The ejected polymer fibers were collected on a drum covered with aluminum foil and rotating at 2000 rpm. The distance between the collector and the needle tip was set at 26 cm. During the process, the relative humidity and temperature were maintained at the constant values of 35% and 20 °C, respectively, by using a custom double chamber with environmental control. The as-spun CoP(3DDT)-(C_{60}HT)/PEO nanofibers were treated by dipping the samples five times in 25 mL of isopropanol for 60 min at 75 °C to remove PEO and obtain pure CoP(3DDT)-(C_{60}HT) nanofibers.

CoP(3DDT)-(C_{60}HT) Nanofiber Characterization. The thermogravimetric analysis (TGA) was conducted using a TA Instruments 2050 which operates under a nitrogen atmosphere, heating the samples from 25 to 800 °C at a scan rate of 10 °C min^{-1}. A TA Instruments 2920 was used for the differential scanning calorimetry (DSC) analysis of polymer samples by changing the temperature from 25 to 250 °C at a rate of 10 °C min^{-1} under a nitrogen atmosphere. DSC results were analyzed using Origin 8 software, and melting temperatures were defined by the peak maximum. X-ray diffraction (XRD) measurements were performed using a Bruker D8 Discover diffractometer with Cu Kα radiation (wavelength of 1.542 Å) operating at 40 kV and 40 mA. The angular range of measurements, 2θ, was between 4° and 30° with a step of 0.01° and time of data accumulation at a particular angular point of 0.2 s. The analysis of electrospun nanofiber morphology was performed using a scanning electron microscope (SEM, JEOL JSM-6390LV) instrument at accelerating voltage of 10 kV. Prior to observations, samples were coated with a thin gold layer. To evaluate the average diameter, 100 individual nanofibers were measured by ImageJ software using SEM images from at least five different sections of each sample. Nanofiber surface topographies were collected by an atomic force microscope (AFM, Ntegra, NT-MDT) equipped with a super sharp silicon cantilever (SSS-NCHR, Nanosensors) and operating in tapping mode. The analyzed nanofibers were first collected onto glass slides and subsequently treated with isopropanol, so that each would release the sacrificial polymer. Single nanofiber mechanical property analyses were performed using the same AFM setup and indenting the already-analyzed nanofiber areas. Elastic moduli were calculated by fitting the loading curves into the Hertz model. Results were obtained by averaging at least 50 indentation curves per sample, acquired by analyzing different nanofibers. Ultraviolet−visible (UV−vis) spectra of CoP(3DDT)-(C_{60}HT) film and nanofibers were recorded on a PerkinElmer Lambda 19 spectrophotometer using films cast on quartz slides from a solution of polymers in *o*-dichlorobenzene and a nanofiber suspension in cyclohexanone (5 mg/mL) using the doctor blading technique.

Photovoltaic Cell Fabrication. Photovoltaic cells were prepared according to the following procedure: the ITO glass substrate (1 cm × 1 cm, surface resistance 20 Ω/sq) was etched on one side by using a 10 wt % aqueous solution of HCl and heated at 60 °C for 15 min to obtain a final area of 0.5 × 1 cm covered by indium tin oxide. The glass was then cleaned in an ultrasonic bath (Elmasonic S30H) using acetone and treated at 60 °C for 20 min with an oxidizing solution (1 mL of aqueous 33 wt % NH_3, 20 mL of distilled water, 4 mL of 30 wt % H_2O_2), washed with distilled water and 2-propanol, and dried with a gentle nitrogen flow. After this treatment, the final resistance of the ITO glass was 12 Ω/sq. Poly(3,4-ethylenedioxythiophene):polystyrenesulfonic acid (PEDOT:PSS; 2.8 wt % dispersion in water, viscosity 20 cP) was diluted 1:1 v/v with 2-propanol and homogenized under mild sonication, filtered on a Gooch G2, and

DOI: 10.1021/acs.macromol.7b00857
Macromolecules 2017, 50, 4972−4981

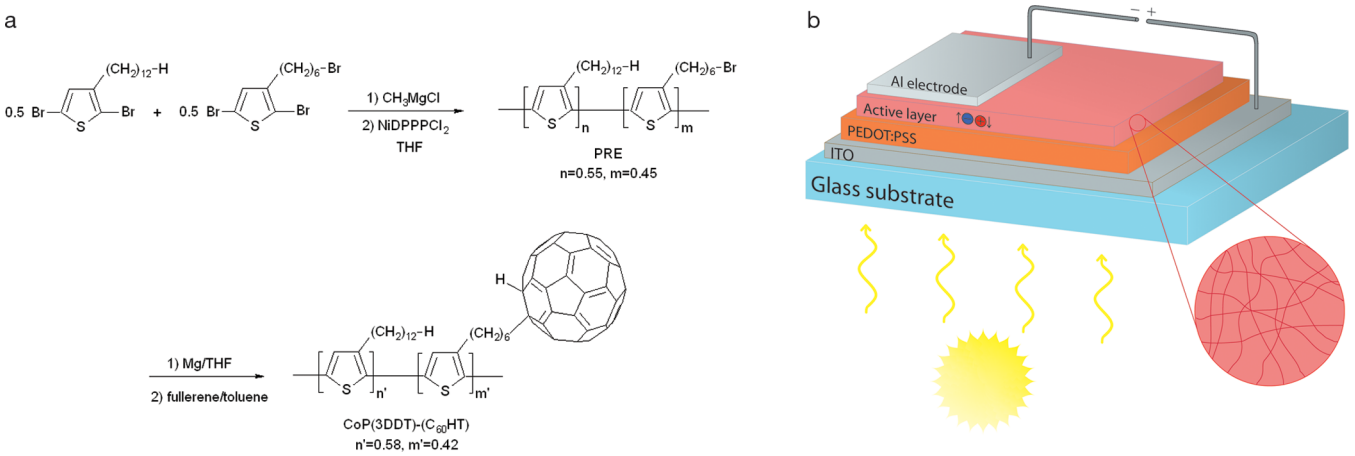

Figure 1. Copolymer structure and device architecture. (a) Synthesis of CoP(3DDT)-(C_{60}HT). Fullerene molecules are inserted into the hexyl side chains of the presynthesized PRE via bimolecular nucleophilic substitution reaction. (b) Schematic representation of the single-material organic solar cell cell structure: indium tin oxide (ITO)/poly(3,4-ethylenedioxythiophene):polystyrenesulfonic acid (PEDOT:PSS)/active layer/aluminum (Al). Photovoltaic measurements are obtained by measuring current and voltage between the ITO anode and the aluminum cathode.

the resulting solution (viscosity 12 cps) was deposited on the previously treated ITO glass via the doctor blading technique using a Sheen Instrument model S265674, leaving only a small 0.5 × 0.5 cm area uncovered on the opposite side of the previously etched area. The PEDOT:PSS film was heated in a Büchi GKR-50 glass oven at 130 °C for 2 h under vacuum. A solution of 5 mg of CoP(3DDT)-(C_{60}HT) in 1 mL of chlorobenzene (or a 5 mg dispersion of CoP(3DDT)-(C_{60}HT) fibers in 1 mL of cyclohexanone) was deposited by doctor blading on the glass slide to cover the PEDOT:PSS layer. A backfill layer was deposited on the fiber layer by doctor blading using the CoP(3DDT)-(C_{60}HT) solution in chlorobenzene. The buffer and active layers were deposited under a nitrogen atmosphere operating inside a MBraun MB 150-GII drybox equipped with H_2O and O_2 analyzers. The annealed samples were heated at 130 °C for 15 min in the Büchi GKR-50 micro glass oven at 10^{-3} mmHg. Lastly, a 50 nm thick Al electrode was deposited over the polymeric layer using an Edwards 6306A coating system operating at 10^{-6} mmHg. The active area of 0.0625 cm^2 of the devices was defined by the area of deposited Al electrode through a shadow mask.

Solar Cell Measurements. The prepared solar cells were stored under nitrogen and in the dark until just before the performance testing procedure. The current−voltage characteristics were measured in air at room temperature using a Keithley 2401 source meter under the illumination of an Abet Technologies LS150 Xenon Arc Lamp Source AM1.5 Solar Simulator, calibrated with an ILT 1400-BL photometer. The photovoltaic performance of the devices exposed to air and light at room temperature was measured every 7 days up to 42 days in order to investigate their stability. Single carrier devices were prepared, and the space-charge limited current (SCLC) was measured to obtain the value for hole mobility (μ) according to the method described by Azimi et al.[14] These devices consisted of a ITO/PEDOT:PSS bottom electrode and an Al top electrode. The CoP(3DDT)-(C_{60}HT) fibers active layer and the electrodes were deposited in the same way as in SMOC devices. The SCLC region was measured applying sufficiently large potentials to study the J−V behavior in the voltage range from 0 to 6 V. Layer thickness and surface features were measured using AFM in a noncontact tapping mode. The reported PCE results were the averaged values obtained from at least ten different devices prepared under the same operative conditions. The spectral responses of the solar cells in the 300−800 nm wavelength range were measured using a SCSpecIII (SevenStar Optics) external quantum efficiency setup.

RESULTS AND DISCUSSION

Synthesis and Characterization of CoP(3DDT)-(C_{60}HT). The chemical structure of CoP(3DDT)-(C_{60}HT) and its synthesis are shown in Figure 1a. To maximize the photovoltaic effect, we required a high content of electron-acceptor groups to be present in the polymer chain.[15] On the other hand, the presence of high quantities of fullerene groups (i) affects polymer solubility, which limits their processability, and[16] most importantly (ii) reduces the macromolecule packing by decreasing chain planarity.[17] We have extensively studied this effect on double-cable polymers, reaching the highest PCE value reported in the literature for SMOCs.[13,15] The already synthesized poly[3-hexylthiophene-*co*-3-(6-fullerenylhexyl)-thiophene] is used as a good starting point for our study.[13] The aim of the proposed synthetic route is to enhance the solubility of the previously synthesized double-cable polymer with high fullerene content in order to enable the occurrence of the electrospinning process.

The synthesis is divided into two main steps. First, regioregular poly[3-dodecylthiophene-*co*-3-(6-bromohexyl)-thiophene] (PRE) was synthesized through a Grignard metathesis (GRIM) reaction followed by Ni(II)-catalyzed polymerization. A typical postpolymerization functionalization (PPF) was then performed on the polymeric precursor PRE in order to insert the fullerenic substituent into its side chains by a bimolecular nucleophilic substitution (S_N2) reaction involving terminal bromine atoms.

The proposed efficient and selective reaction produces well-defined polymer chains with high fullerene content. ^{1}H NMR spectroscopy (Figure S1) was used to estimate the PRE degree of regioregularity (95% in head-to-tail dyads, HT) by evaluating the integral ratio of the signal centered at 2.65 ppm (HT dyads) with that at 2.45 ppm (non HT dyads). PRE composition (3-dodecylthiophene:3-(6-bromohexylthiophene) 0.55:0.45 molar ratio) was found by comparing the integral of the signal of the methyl group belonging to the dodecylic monomer at 0.93 ppm with the integral of the triplet at 3.43 ppm ascribable to the α-methylenic protons to the −Br group. The high degree of regioregularity (95% in head-to-tail dyads) of CoP(3DDT)-(C_{60}HT) was determined by evaluating the integral ratio of the signal at 6.98 (HT-HT triads) with those at 7.01 and 7.03 ppm (non HT-HT triads) in the ^{1}H NMR spectrum (Figure S2). The composition of CoP(3DDT)-(C_{60}HT) slightly differs from that of PRE since the postpolymerization functionalization is not quantitative, having an 85% yield. So it can be argued that

DOI: 10.1021/acs.macromol.7b00857
Macromolecules 2017, 50, 4972−4981

the recovered more soluble portion of the fullerenated polymer was made of polymeric chains with a higher alkylic monomer content. The sequence of the two comonomers in the copolymers is not directly evaluable from their ^{1}H NMR spectra. However, considering that the two dibrominated intermediates 2,5-dibromo-3-dodecylthiophene and 2,5-dibromo-3-(6-bromohexyl)thiophene only differ by their various side chain lengths (since the electron-withdrawing group −Br is electronically separated from the thiophenic ring by the oligomethylenic spacer), it is reasonable to suppose that they have a similar reactivity toward the polymerization reaction. This is also confirmed by the obtained PRE composition value 3-dodecylthiophene:3-(6-bromohexyl)thiophene) molar ratio of 0.55:0.45) which is similar to the monomers feed ratio value (0.5:0.5). In view of this, we hypothesize that the copolymers have a random sequence arrangement of the two monomers.

FT-IR spectra of polymers before and after the PFP reaction highlighted the chemical bonding of fullerene (four IR absorption peaks at 1429, 1173, 577, and 526 cm^{-1}) (Figure S3 and Table S1).[18,19] The final composition of 3-dodecylthiophene:3-(6-fullerenylhexyl)thiophene copolymer (0.58:0.42 molar ratio) was determined by comparing the integral of the ^{1}H NMR signal of the methyl group belonging to the alkylic monomer at 0.92 ppm with the integral of the peak at 3.45 ppm, ascribable to the methylene group directly linked to fullerene, which is present only in the functionalized monomer. The high regioregularity degree is fundamental for guaranteeing well-ordered polymers with close $\pi-\pi$ stacking, which is necessary to maximize the charge mobility.[20]

GPC results revealed the high number-average molecular weight (M_n) of CoP(3DDT)-(C_{60}HT), which was 48 000 Da with a narrow polydispersity index (PDI) of around 1.2 (Figure S4). Moreover, the presence of a dodecyl group in the copolymer structure strongly increased its solubility up to 30 mg/mL in chloroform.

In order to fabricate SMOCs with high efficiency, the proposed copolymer synthesis was optimized before the production of the devices by studying the effect of the copolymer monomer ratio on the solar cell performance. To this end, CoP(3DDT)-(C_{60}HT) with four different monomer ratios was synthesized and used to fabricate SMOCs (without incorporating electrospun nanofibers) according to the protocol shown in this article. The annealed device obtained by using CoP(3DDT)-(C_{60}HT) with molar ratio of 85:15 had a PCE of 2.58%. The SMOC fabricated by using the copolymer with molar ratio of 70:30 gave a significant enhancement of photovoltaic performance (PCE = 2.90%). The best result was achieved fabricating SMOC with CoP(3DDT)-(C_{60}HT) with molar ratio of 58:42 which led an increase in performance of about 34% in terms of PCE (3.47%) when compared to the lowest fullerene content cell. Photovoltaic tests on devices fabricated clearly confirmed that SMOC performance improves when increasing the fullerene content in the copolymer. On the other hand, increasing the monomer ratio up to 50:50 CoP(3DDT)-(C_{60}HT) showed poor solubility which did not allow the fabrication of stable SMOCs as a result of macroscale polymer aggregation.

Electrospinning of CoP(3DDT)-(C_{60}HT) Nanofibers. To fabricate CoP(3DDT)-(C_{60}HT) nanofibers, first we electrospun a chloroform solution of CoP(3DDT)-(C_{60}HT) (3.3 wt %) and PEO (0.7 wt %). The presence of flexible insulating polymer chains helps the formation of uniform nanofibers with a self-organized core−shell structure.[21] Previous studies have already successfully demonstrated that due to the different viscosity, CoP(3DDT)-(C_{60}HT) molecules are placed in the inner part of the nanofiber.[21] Nanofibers were then treated a few times with isopropanol at 75 °C, in order to selectively etch out PEO and obtain pure CoP(3DDT)-(C_{60}HT) nanofibers.

First we determined the PEO removal efficiency by TGA. The blend nanofiber thermogram showed two different signals, confirming the presence of both polymers, while the CoP-(3DDT)-(C_{60}HT) nanofiber curve did not show the PEO-related weight loss (Figure S5). The treated nanofiber TGA curve thermogram showed features similar to those of the as-synthesized copolymer thermogram. In agreement with several previous articles, we found that the chemical etching performed at a temperature above the PEO melting temperature encourages the complete chemical removal of PEO from polythiophene derivative electrospun nanofibers.[21] Moreover, the final percentage weight detected (around 40%) is consistently higher than that of regular poly(3-alkylthiophene)-s. This discrepancy confirms the chemical grafting of a large number of fullerene groups to the polymer chains.[22]

Electrospun materials were characterized by SEM and AFM to investigate both mat and single-fiber morphology. Figures 2a and 2b show electrospun nanofibers which were made from a blend solution before and after PEO etching, respectively. The images reveal CoP(3DDT)-(C_{60}HT)/PEO cylindrical fibers with nanoscale diameters (0.93 ± 0.08 μm). Nanofibers are uniform and characterized by the typical polythiophene derivative/PEO textured surfaces.[23] Etching out PEO generates pure CoP(3DDT)-(C_{60}HT) with a 0.85 ± 0.12 μm diameter. The volumetric reduction is consistent with the amount of PEO used to spin nanofibers (17.5%), and moreover, PEO removal does not cause any substantial worsening in the material morphology.

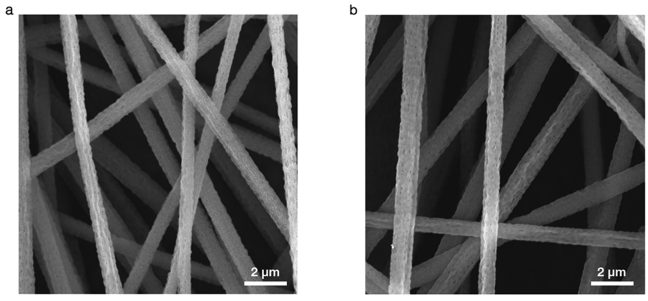

Figure 2. Electrospun mat morphology. (a) SEM image of CoP(3DDT)-(C_{60}HT)/PEO blend fibers. (b) SEM micrograph of CoP(3DDT)-(C_{60}HT) fibers when PEO was removed by washing the fiber mat with isopropanol at 75 °C.

Post-treated nanofibers show continuous and well-defined structures, although nanofiber surfaces appear more irregular and dotted, as demonstrated by AFM topographies (Figures 3a,b). The polka-dot surface is due to the removal of PEO. The insulator polymer was located on the external part of the blend nanofibers and tended to form nanoscale domains. The surface corrugation and the presence of small holes are visible in SEM micrographs as well as in the rise in the standard diameter deviation. Moreover, electrospinning generates considerable improvements in terms of CoP(3DDT)-(C_{60}HT) material mechanical properties.[24] By using AFM nanoindentation, it was seen that the elastic modulus values rise considerably from 1.59

DOI: 10.1021/acs.macromol.7b00857
Macromolecules 2017, 50, 4972−4981

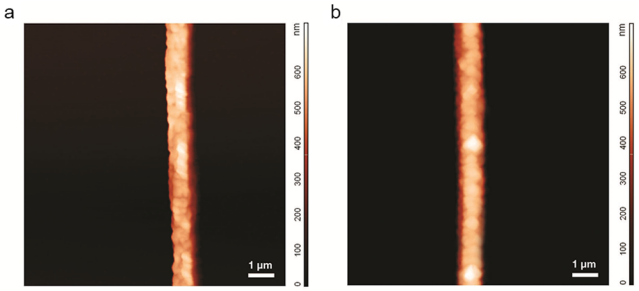

Figure 3. Morphological surface properties of single electrospun nanofibers. (a) Single fiber AFM topographical image of the as-spun blend. (b) AFM topography image of the surface of a single CoP(3DDT)-(C_{60}HT) nanofiber after etching the PEO phase out of the blend.

± 0.16 to 2.52 ± 0.31 GPa analyzing film and single fibers of CoP(3DDT)-(C_{60}HT).[25,26]

Polymer crystallinity was first investigated by DSC, analyzing electrospun CoP(3DDT)-(C_{60}HT) as well as a thin film of the same polymer as a reference (Figure 4a and Table 1). The DSC thermogram of the CoP(3DDT)-(C_{60}HT) film shows an endothermic flexure at 52 °C (T_g, glass transition temperature) and two endothermic peaks (melting temperatures T_{m1} and T_{m2}) at 122 and 225 °C, which can be ascribed to the melting of crystalline domains determined by the packing of side chains and backbone, respectively.[13] It also shows an evident exothermic crystallization peak at 148 °C (T_c). The DSC thermogram of CoP(3DDT)-(C_{60}HT) fibers is quite similar but evidences a lower T_{m1} temperature, related to the different spatial disposition of the side chains when electrospun in fibers. The nanofiber formation process involves a fast solvent evaporation that affects the side chain arrangement, as confirmed by a slight decrease in the first melting signal enthalpy (ΔH_{m1}) of the fibers. Electrospinning has a marked impact on the stretching and alignment of polymer backbone chains, which is highlighted by the increment ΔH_{m2} in the nanofiber sample.

XRD (Figure 4b) tests were conducted to further investigate the inner nanofiber structure. The XRD scans of CoP(3DDT)-(C_{60}HT)/PEO and CoP(3DDT)-(C_{60}HT) nanofibers show the typical semicrystalline diffraction peak of PEO signal (2θ = 19.1°) only in the first sample, thus confirming the etching process effectiveness.[27] The (100) reflection due to the CoP(3DDT)-(C_{60}HT) lamellar structures (2θ = 5.1°) became sharper after the postelectrospinning process, thus indicating the development of well-structured copolymer crystallites when fibers were exposed to the organic solvent at high temperature.[26] The (010) peak 2θ = 23.5° indicates that the $\pi-\pi$ interaction is not present in the CoP(3DDT)-(C_{60}HT) film diffractogram, while it is well visible in the spun materials, indicating that CoP(3DDT)-(C_{60}HT) undergoes backbone chain alignment during the electrospinning process, which promotes the interchain $\pi-\pi$ stacking and crystallization.[26] Lastly, it is worth noting the absence of any fullerene aggregation-related peaks. The formation of large fullerene aggregates, which is one of the main causes of poor SMOC performance, has been avoided thanks to the presence of an alkyl spacer between the fullerenes and the backbone.[22]

Optical absorption profiles (Figure 4c) show significant enhancements with regard to material–light interactions after the polymer chain arrangements via electrospinning. UV–vis

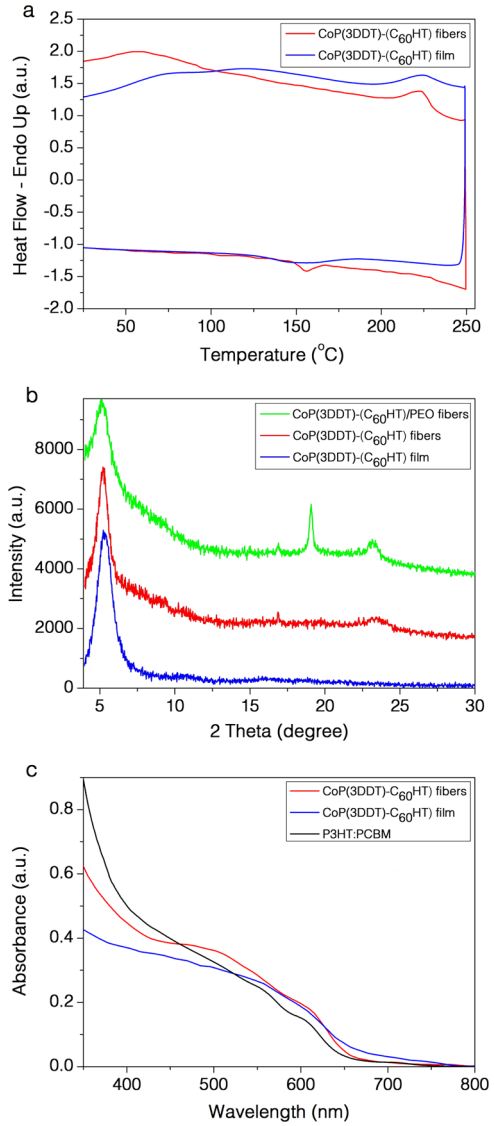

Figure 4. Chemical structure characterization reveals molecular order in electrospun one-dimensional nanomaterials. (a) DSC thermograms of polymer CoP(3DDT)-(C_{60}HT) fibers and film under dynamic nitrogen atmosphere at a heating rate of 10 °C min^{-1}. The upper lines are collected from heating scans and the lower lines from cooling scans. (b) XRD scattering patterns from CoP(3DDT)-(C_{60}HT) film, fibers, and CoP(3DDT)-(C_{60}HT)/PEO blend fibers recorded in a range of 2θ from 4° to 30°. (c) Comparison of optical absorption spectra of CoP(3DDT)-(C_{60}HT) film and nanofibers as well as of a film of a P3HT:PCBM physical mixture typically used for BHJ solar cells.

Table 1. Thermal Properties of CoP(3DDT)-(C_{60}HT) Film and Electrospun Nanofibers Obtained by Differential Scanning Calorimetry; Glass Transition (T_g), Melting Points (T_m), Crystallization Points (T_c), and Thermal Transition Enthalpies (ΔH_m and ΔH_c) Are Indicated

sample	T_g (°C)	T_{m1} (°C)	T_{m2} (°C)	T_c (°C)	ΔH_{m1} (J/g)	ΔH_{m2} (J/g)	ΔH_c (J/g)
CoP(3DDT)-(C_{60}HT) film	52	122	225	148	3.12	5.29	4.62
CoP(3DDT)-(C_{60}HT) fibers	46	120	223	156	0.81	7.40	3.71

DOI: 10.1021/acs.macromol.7b00857
Macromolecules 2017, 50, 4972–4981

spectra of both CoP(3DDT)-(C_{60}HT) samples show (i) an absorbance in the area around 350 nm, which may be ascribed to fullerene derivatives in side chains (more evident in the fiber sample), and (ii) a peak around 500 nm, which may be attributed to the polythiophenic system $\pi-\pi^*$ transition. The presence in the electrospun fibers of a further shoulder at around 620 nm—which is usually assigned to noninterdigitating crystalline domains—indicates the formation of $\pi-\pi$ stacking between thiophene rings.[28] Furthermore, the absorption shoulder at 620 nm reflects a significant planarization of the polythiophene backbone chains and interchain aggregation at the nanoscale range. This spectral feature, which is similar to that observed in other donor/acceptor polythiophene copolymers films, arises from the solvent evaporation during the preparation of solid state samples.[17]The CoP(3DDT)-(C_{60}HT) nanofiber UV−vis spectrum shows enhanced absorption even when compared to typical poly(3-hexylthiophene) and [6,6]-phenyl C_{61}-butyric acid methyl ester (P3HT:PCBM) BHJs system films with weight ratio of 1:1. The red-shift in nanofiber absorption peaks suggests that polymer chains have a more extended conformation and better delocalized π-conjugation.[29] Moreover, the red-shift allows the $\pi-\pi^*$ transition to fit perfectly with the wavelength of the maximum solar spectrum, providing an improved overlap with the solar emission while increasing the final efficiency of photovoltaic cells.

Single-Material Organic Solar Cell Fabrication and Performance. The final solar cells used here have the same architecture that we have always used for studying the active material properties with preoptimized layer thickness: indium tin oxide (ITO)/poly(3,4-ethylenedioxythiophene):polystyrenesulfonic acid (PEDOT:PSS)/active layer/aluminum (Al) (Figure 1b).[13,15,30] Glass slides covered by 80 nm of ITO were used as the support for fabricating cells. A PEDOT:PSS layer (120 nm) was deposited onto the ITO surface. Active layers with a 120 nm thickness were laid by the doctor blading technique, and last, 50 nm thick Al layer cathodes were deposited by thermal evaporation. CoP(3DDT)-(C_{60}HT) fiber solar cells were characterized as prepared and after thermal annealing (see Experimental Section for cell fabrication details). To embed the electrospun nanofibers into the active layer, materials were deposited according to a method developed by the Steckl research group.[31] This procedure is divided into two stages. First, a layer of CoP(3DDT)-(C_{60}HT) fibers was deposited onto the ITO/PEDOT substrate, and then a backfill layer was deposited on the fibers by doctor blading, using a fully solubilized CoP(3DDT)-(C_{60}HT) solution. The second part of the process is fundamental for interconnecting fibers and creating a uniform layer. The use of an unsaturated solution allows for a further nanofibers diameter reduction while maintaining the structure that serves as a template for the fully solubilized CoP(3DDT)-(C_{60}HT) during the construction of the final layer. It is well-known that in electrospun conjugated polymer materials the inner portion of the fibers has polymer chains that are more aligned and closely packed, with improved crystallinity compared to the nanofiber external region.[32] Therefore, nanomaterial−light interaction, charge transport, and mechanical properties can be enhanced by the dissolution of the CoP(3DDT)-(C_{60}HT) fiber external layer.

The photovoltaic performance of this device was compared to that of a SMOC prepared with a CoP(3DDT)-(C_{60}HT) film (with no fibers) as the active layer, and one type of conventional BHJ device fabricated by using a 1:1 P3HT:PCBM weight ratio blend, in order to investigate the origin of the improvements in the SMOCs incorporating nanofibers.

The morphology of the final cell active layers after the annealing process was examined by using tapping mode AFM height and phase images (Figure 5) in order to evaluate the influence of the inclusion of nanofibers in the structure of the active material. Both height images (Figures 5a,c) show flat surfaces with root-mean-square roughness of around 1 nm. The morphology of the film without electrospun nanofibers is more regular than that of fiber-based active materials. The presence of electrospun nanofibers within the cell active layer leads to a slight increment in roughness, confirming the result previously found by Bedford et al.[31] The phase images (Figures 5b,d) reveal the absence of large fullerene aggregates in both analyzed materials and a significant variation in the active layer structure caused by the addition of electrospun nanofibers. The CoP(3DDT)-(C_{60}HT) active layer without fibers shows a featureless phase image, while the presence of a nanopattern is clearly visible in the layer with incorporated electrospun fibers. The nanopattern formation is often related to the development of higher efficiency devices. Moreover, it is important to mention that several similar diblock copolymers show a typical fibrous-like structure due to the separation of the crystalline polythiophene block and the fullerene-attached blocks.[33] The CoP(3DDT)-(C_{60}HT) active layer structure has a more spherical morphology due to the large number of fullerene groups present within the polymer. Similar results were found by Miyanishi et al. when studying the relationship between the amounts of the attached fullerene and the nanopattern morphology, which proved that large fullerene volumes strongly disturb the fibril formation leading to more spherical patterns and to higher device performances.[34]

Figure 6a shows the current density versus the voltage ($J-V$) characteristics of solar cells with different active layer

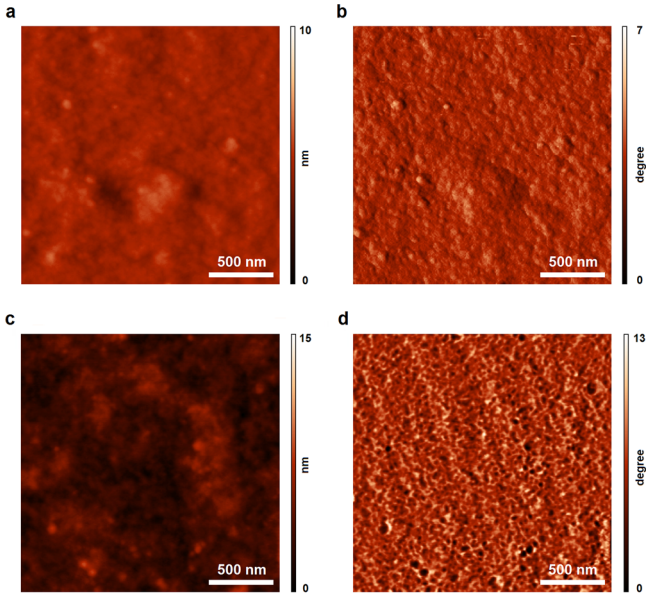

Figure 5. Active layer surface structure of CoP(3DDT)-(C_{60}HT) SMOCs. AFM topographical (left) and phase images (right) of SMOC active materials from (a, b) an annealed film of CoP(3DDT)-(C_{60}HT) and (c, d) an annealed CoP(3DDT)-(C_{60}HT) layer incorporating electrospun nanofibers.

DOI: 10.1021/acs.macromol.7b00857
Macromolecules 2017, 50, 4972−4981

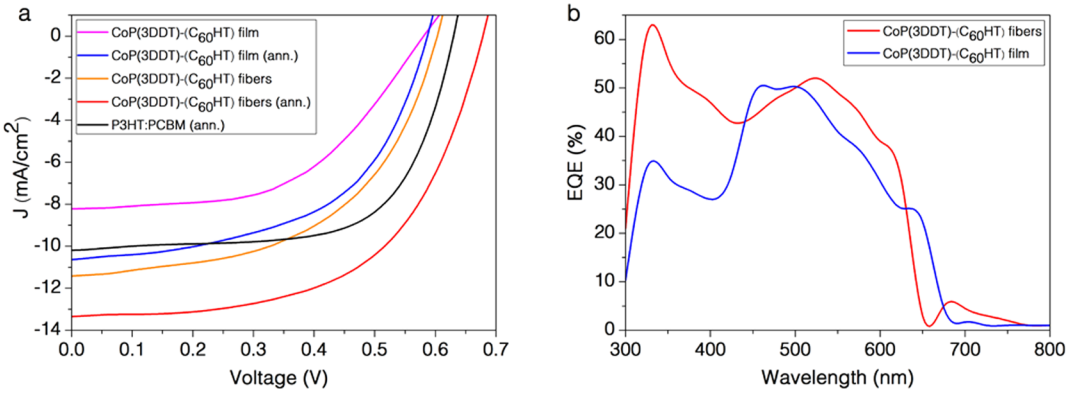

Figure 6. Performance of CoP(3DDT)-(C_{60}HT) SMOCs. (a) Current–voltage (J–V) characteristics of different CoP(3DDT)-(C_{60}HT) devices and a P3HT:PCBM BHJ solar cell under simulated AM1.5G sunlight illumination. (b) EQE spectra of the thermally treated SMOCs fabricated using a thin layer of CoP(3DDT)-(C_{60}HT) and introducing CoP(3DDT)-(C_{60}HT) nanofibers into the active material.

composition and structure under illumination of an air mass (AM) 1.5 solar simulator. In order to evaluate the effect of the presence of nanofibers as a template within the active layer, we evaluated the efficiency of the devices fabricated with a simple CoP(3DDT)-(C_{60}HT) thin layer. Device performances were analyzed before and after annealing in order to evaluate the thermal treatment influence. Additionally, the efficiencies of the SMOCs were compared by using the P3HT:PCBM cell as a standard reference to assess the performance of the optimized photovoltaic cells. As for the quantitative comparison, Table 2 and Table S2 show the best and average photovoltaic parameters for all those devices, respectively.

Table 2. Best Photovoltaic Device Performance of the BHJ Reference Cell and SMOCs with Different Active Layer Structures and Thermal Treatments

sample	J_{sc} (mA cm^{-2})	V_{oc} (V)	FF (%)	PCE (%)
P3HT:PCBM (annealed)	10.1	0.63	56	3.55
CoP(3DDT)-(C_{60}HT) film	8.2	0.58	51	2.43
CoP(3DDT)-(C_{60}HT) film (annealed)	10.7	0.59	55	3.47
CoP(3DDT)-(C_{60}HT) fibers	11.4	0.60	55	3.76
CoP(3DDT)-(C_{60}HT) fibers (annealed)	13.3	0.68	62	5.58

The P3HT:PCBM device had a short-circuit current density (J_{sc}) of 10.1 mA cm^{-2}, an open circuit voltage (V_{oc}) of 0.63 V, a fill factor (FF) of 56%, and a PCE of 3.55%. These results are consistent with the best value reported in the literature for the conventional BHJ solar cell architecture made with this blend[35] as well as with our previous results.[13] Solar cells made with a CoP(3DDT)-(C_{60}HT) film and annealed showed a similar PCE to that of the BHJ device, thus highlighting the potential benefits of SMOCs. The high fullerene content within the diblock copolymer and the direct chemical attachment of fullerene-containing groups to the polymer backbones make it possible to reach the BHJ percolation threshold and achieve a similar photovoltaic efficiency. In this respect, it is worth remembering that the potential for scaling-up OSC fabrication is affected by the active material costs; therefore, the development of devices with appropriate efficiency and low content of fullerene will play a fundamental role for the possible industrial future of these devices.[4] It is well-known that the open-circuit voltage value defines the transfer process from the generation of excitons to the carrier collection. The V_{oc} value depends on the effective donor/acceptor bandgap and is significantly affected by the carrier's recombination.[36] The V_{oc} values of the BHJ reference and SMOCs are approximately at the same level, which proves that it is possible to overcome one of the main double-cable polymer limitations caused by the charge recombination using the proposed chemical synthesis strategy.[37] Furthermore, we proved that it is possible to exceed the open-circuit voltage BHJ threshold by incorporating nanofibers into the active layer.

A significant improvement in terms of performance was achieved by including the nanostructured template into the device. Among the developed devices, the one with the best performance showed a PCE of 5.58%, with a hole mobility of 8.4×10^{-4} cm^2 V^{-1} s^{-1}, FF of 62%, V_{oc} of 0.68 V, and J_{sc} of 13.3 mA cm^{-2} when the CoP(3DDT)-(C_{60}HT) fiber cell was thermally annealed. To the best of our knowledge, this is the highest power conversion efficiency reported for a SMOC. The effect of the thermal treatment on the photovoltaic performance of the device was clearly visible. These improvements are attributed to more favorable stacking interactions and side-group disposition, permitting a more balanced charge transport.[38]

As displayed in Figure S6, the efficiency level of the fabricated SMOCs exhibits good stability when exposed to ambient conditions. It can be clearly observed that their performance decreases rapidly in the first few days and more slowly afterward. The fiber-containing samples were more stable than the corresponding ones in film state: the most stable sample was that of CoP(3DDT)-(C_{60}HT) fibers (annealed) while the less stable was that of CoP(3DDT)-(C_{60}HT) film, and their PCE decreased by 16.7% and 37.9%, respectively, from their initial values in 42 days. Annealed CoP(3DDT)-(C_{60}HT) fiber SMOC test shows an initial efficiency drop-off followed by a slower degradation which leads to a PCE value of 4.65%, confirming that these cells maintain high efficiency over a long period of time.

To further investigate the mechanism responsible for the performance enhancement, we analyzed the external quantum efficiency (EQE) of the annealed devices (Figure 6b) under 1 sun illumination. The curve related to the device based on CoP(3DDT)-(C_{60}HT) in film form showed three feature peaks at 333, 462, and 499 nm plus three shoulders at 378, 573, and 637 nm. The device based on copolymer fibers showed two main peaks at 332 and 525 nm, plus three shoulders at 395,

DOI: 10.1021/acs.macromol.7b00857
Macromolecules 2017, 50, 4972–4981

570, and 615 nm, accompanied by a peak of small intensity centered at 685 nm. The EQE profiles follow the absorption spectra trend, thus demonstrating that the harvested photons contribute directly to the photocurrent and confirming the lowering of the recombination side effects. Enhanced quantum efficiency was observed in the device made with CoP(3DDT)-(C_{60}HT) fibers as compared to the device made with CoP(3DDT)-(C_{60}HT) film, showing the improved charge collection efficiency of the former. Maximum EQE in the CoP(3DDT)-(C_{60}HT) fibers reached 61% at around 330 nm, which is remarkably higher (+12.5%) than the most intense peak in the SMOCs prepared without fiber. This peak is ascribed to the $\pi-\pi^*$ transition of chromophoric fullerene derivatives in the side chain.[39] This result highlighted the beneficial effect of the method used on the conformation of both backbone and side polymer chains. Furthermore, a significant improvement in quantum efficiency was observed in the 500−625 nm wavelength region, which corresponds to the maximum spectral zone of the solar radiation hitting the Earth's surface. The enhanced polymer structure also influences other parameters so that CoP(3DDT)-(C_{60}HT) fiber SMOCs achieve a higher fill factor, consistent with a higher degree of polymer chain ordering and interchain $\pi-\pi$ stacking.[40] Lastly, the J_{sc} of fiber cells is greater than that of the film cells, which arise from the greater photocurrent generated in the 300−625 nm region.

CONCLUSIONS

We report on the development of a novel SMOC with power conversion efficiency as high as 5.58% which, to the best of our knowledge, is the highest value reported so far for a single material device. The newly synthesized donor−acceptor polymer (CoP(3DDT)-(C_{60}HT)) with high fullerene group content, high regioregularity, and great solubility may contribute to a greater charge carrier mobility and lower charge recombination, mutually accountable for open-circuit voltage greater than those of a conventional BHJ blend and previously developed single-material devices. Moreover, the presence of the electron-acceptor group chemically linked to the main chain by the alkyl spacer makes it possible to prevent phase-separation phenomena, even at a high fullerene content. Electrospun CoP(3DDT)-(C_{60}HT) nanofibers were found to have a degree of polymer chain order which is conducive to interchain $\pi-\pi$ stacking and the development of well-structured copolymer crystallites. These features contribute to a more efficient UV−vis radiation absorption, the creation of ideal pathways for charge carriers, and improved mechanical properties. The inclusion of nanofibers in the SMOC as a template and thermal annealing strongly contribute to the optimization of the active material structure, leading to an increase in both the external quantum efficiency and cell photovoltaic properties. The great efficiency improvement confirms that the design of innovative macromolecules should be synergistically supported by the development of a well-defined hierarchical architecture which takes into account the polymer supramolecular arrangement and active layer nanostructuration in order to obtain high-performance SMOCs.

These findings open up new design solutions for novel organic solar cells. Furthermore, the achieved efficiency improvements, +57.2% compared to those of the BHJ reference cells, reveal the potential of CoP(3DDT)-(C_{60}HT) devices for photovoltaic applications.

ASSOCIATED CONTENT

Supporting Information

The Supporting Information is available free of charge on the ACS Publications website at DOI: 10.1021/acs.macromol.7b00857.

^{1}H NMR spectrum of PRE; ^{1}H NMR spectrum of CoP(3DDT)-(C_{60}HT); FT-IR spectra of PRE and CoP(3DDT)-(C_{60}HT); FT-IR absorption bands and signal assignments for PRE and CoP(3DDT)-(C_{60}HT); GPC trace of CoP(3DDT)-(C_{60}HT); TGA curves of the electrospun nanofibers before and after postproduction treatment; summary of photovoltaic response data of the BHJ reference cell and different SMOCs; SMOCs efficiency as a function of device storage time (PDF)

AUTHOR INFORMATION

Corresponding Author

*E-mail: fpierini@ippt.pan.pl (F.P.).

ORCID

Filippo Pierini: 0000-0002-6526-4141

Author Contributions

F.P. and M.L. conceived and developed the ideas. M.L. performed CoP(3DDT)-(C_{60}HT) synthesis and characterization (^{1}H NMR, FT-IR, GPC, and UV−vis). F.P. and P.N. designed and conducted electrospinning experiments. O.U. carried out SEM, DSC, and XRD measurements. S.P. performed TGA analysis. F.P. and K.Z. acquired and processed AFM data. M.L. fabricated and tested photovoltaic devices. F.P. wrote the manuscript. All authors discussed results and commented on the manuscript. T.A.K supervised the project.

Notes

The authors declare no competing financial interest.

ACKNOWLEDGMENTS

This work was supported by the National Science Centre grant no. 2015/19/D/ST8/03196. Experiments were performed using equipment made available thanks to EC structural funds (project POIG no. 02.02.00-17-024/08-00). Some support was also received from the Selected Topics Research Fund of the University of Bologna. In particular, the authors thank P. Sajkiewicz for his assistance with nanofiber characterization. Insightful discussions with J. Roncali were also greatly appreciated.

ABBREVIATIONS

SMOC, single-material organic solar cell; OSC, organic solar cell; PCE, power conversion efficiency; BHJ, bulk heterojunction; 1D, one-dimensional; 3D, three-dimensional; CoP(3DDT)-(C_{60}HT), poly[3-dodecylthiophene-*co*-3-(6-fullerenylhexyl)thiophene]; PRE, poly[3-dodecylthiophene-*co*-3-(6-bromohexyl)thiophene]; GRIM, Grignard metathesis; PPF, postpolymerization functionalization; S_N2, bimolecular nucleophilic substitution; HT, head-to-tail; FT-IR, Fourier transform infrared; GPC, gel permeation chromatography; PDI, polydispersity index; ITO, indium tin oxide; PEDOT:PSS, poly(3,4-ethylenedioxythiophene):polystyrenesulfonic acid; Al, aluminum; PEO, poly(ethylene oxide); TGA, thermogravimetric analysis; SEM, scanning electron microscopy; AFM, atomic force microscopy; DSC, differential scanning calorimetry; T_g, glass transition temperature; T_m, melting temperature; T_c, crystallization temperature; ΔH_m, enthalpy of fusion; ΔH_c,

DOI: 10.1021/acs.macromol.7b00857
Macromolecules 2017, 50, 4972−4981

enthalpy of crystallization; XRD, X-ray diffraction; UV−vis, ultraviolet−visible; P3HT, poly(3-hexylthiophene); PCBM, [6,6]-phenyl C_{61}-butyric acid methyl ester; SCLC, space-charge limited current; μ, hole mobility; $J-V$, current density versus voltage; AM, air mass; J_{sc}, short-circuit current density; V_{oc}, open circuit voltage; FF, fill factor; EQE, external quantum efficiency.

REFERENCES

(1) Gunes, S.; Neugebauer, H.; Sariciftci, N. S. Conjugated Polymer-Based Organic Solar Cells. *Chem. Rev.* **2007**, *107*, 1324−1338.

(2) Dennler, G.; Scharber, M. C.; Brabec, C. J. Polymer-Fullerene Bulk-Heterojunction Solar Cells. *Adv. Mater.* **2009**, *21*, 1323−1338.

(3) Li, M.; Gao, K.; Wan, X.; Zhang, Q.; Kan, B.; Xia, R.; Liu, F.; Yang, X.; Feng, H.; Ni, W.; Wang, Y.; Peng, J.; Zhang, H.; Liang, Z.; Yip, H.-L.; Peng, X.; Cao, Y.; Chen, Y. Solution-Processed Organic Tandem Solar Cells with Power Conversion Efficiencies > 12%. *Nat. Photonics* **2016**, *11*, 85−90.

(4) Po, R.; Roncali, J. Beyond Efficiency: Scalability of Molecular Donor Materials for Organic Photovoltaics. *J. Mater. Chem. C* **2016**, *4*, 3677−3685.

(5) Ray, B.; Alam, M. Random vs Regularized OPV: Limits of Performance Gain of Organic Bulk Heterojunction Solar Cells by Morphology Engineering. *Sol. Energy Mater. Sol. Cells* **2012**, *99*, 204−212.

(6) Roncali, J. Linear π-Conjugated Systems Derivatized with C_{60}-Fullerene as Molecular Heterojunctions for Organic Photovoltaics. *Chem. Soc. Rev.* **2005**, *34*, 483−495.

(7) Roncali, J. Single Material Solar Cells: the Next Frontier for Organic Photovoltaics? *Adv. Energy Mater.* **2011**, *1*, 147−160.

(8) Yamamoto, S.; Yasuda, H.; Ohkita, H.; Benten, H.; Ito, S.; Miyanishi, S.; Tajima, K.; Hashimoto, K. Charge Generation and Recombination in Fullerene-Attached Poly(3- hexylthiophene)-Based Diblock Copolymer Films. *J. Phys. Chem. C* **2014**, *118*, 10584−10589.

(9) Cravino, A.; Sariciftci, N. S. Double-Cable Polymers for Fullerene Based Organic Optoelectronic Applications. *J. Mater. Chem.* **2002**, *12*, 1931−1943.

(10) Yarin, A. L.; Pourdeyhimi, B.; Ramakrishna, S. In *Fundamentals and Applications of Micro- and Nanofibers*; Cambridge University Press: Cambridge, 2014.

(11) Kolbuk, D.; Sajkiewicz, P.; Kowalewski, T. A. Optical Birefringence and Molecular Orientation of Electrospun Polycaprolactone Fibers by Polarizing-Interference Microscopy. *Eur. Polym. J.* **2012**, *48*, 275−283.

(12) Lee, S.; Moon, G. D.; Jeong, U. Continuous Production of Uniform Poly(3-hexylthiophene) (P3HT) Nanofibers by Electrospinning and Their Electrical Properties. *J. Mater. Chem.* **2009**, *19*, 743−748.

(13) Lanzi, M.; Salatelli, E.; Benelli, T.; Caretti, D.; Giorgini, L.; Di-Nicola, F. P. A Regioregular Polythiophene−Fullerene for Polymeric Solar Cells. *J. Appl. Polym. Sci.* **2015**, *132*, 42121−42131.

(14) Azimi, H.; Senes, A.; Scharber, M. C.; Hingerl, K.; Brabec, C. J. Charge Transport and Recombination in Low-Bandgap Bulk Heterojunction Solar Cell using Bis-adduct Fullerene. *Adv. Energy Mater.* **2011**, *1*, 1162−1168.

(15) Lanzi, M.; Paganin, L.; Errani, F. Synthesis, Characterization and Photovoltaic Properties of a New Thiophene-Based Double-Cable Polymer with Pendent Fullerene Group. *Polymer* **2012**, *53*, 2134−2145.

(16) Yang, C.; Lee, J. K.; Heeger, A. J.; Wudl, F. Well-Defined Donor−Acceptor Rod−Coil Diblock Copolymers Based on P3HT Containing C_{60}: the Morphology and Role as a Surfactant in Bulk-Heterojunction Solar Cells. *J. Mater. Chem.* **2009**, *19*, 5416−5423.

(17) Ouhib, F.; Khoukh, A.; Ledeuil, J.-B.; Martinez, H.; Desbrieres, J.; Dagron-Lartigau, C. Diblock and Random Donor Acceptor "Double Cable" Polythiophene Copolymers via the GRIM Method. *Macromolecules* **2008**, *41*, 9736−9743.

(18) Li, M.; Xu, P.; Yang, J.; Yang, S. Donor-π-Acceptor Double-Cable Polythiophenes Bearing Fullerene Pendant with Tunable Donor/Acceptor Ratio: A Facile Postpolymerization. *J. Mater. Chem.* **2010**, *20*, 3953−3960.

(19) Nayak, P. L.; Yang, K.; Dhal, P. K.; Alva, S.; Kumar, J.; Tripathy, S. K. Polyelectrolyte-Containing Fullerene I: Synthesis and Characterization of the Copolymers of 4-Vinylbenzoic Acid with C_{60}. *Chem. Mater.* **1998**, *10*, 2058−2066.

(20) Guo, J.; Ohkita, H.; Benten, H.; Ito, S. Near-IR Femtosecond Transient Absorption Spectroscopy of Ultrafast Polaron and Triplet Exciton Formation in Polythiophene Films with Different Regioregularities. *J. Am. Chem. Soc.* **2009**, *131*, 16869−16880.

(21) Kim, T.; Im, J. H.; Choi, H. S.; Yang, S. J.; Kim, S. W.; Park, C. R. Preparation and Photoluminescence (PL) Performance of a Nanoweb of P3HT Nanofibers with Diameters Below 100 nm. *J. Mater. Chem.* **2011**, *21*, 14231−14239.

(22) Lee, J. U.; Cirpan, A.; Emrick, T.; Russell, T. P.; Jo, W. H. Synthesis and Photophysical Property of Well-Defined Donor−Acceptor Diblock Copolymer Based on Regioregular Poly(3-hexylthiophene) and Fullerene. *J. Mater. Chem.* **2009**, *19*, 1483−1489.

(23) Laforgue, A.; Robitaille, L. Fabrication of Poly-3-hexylthiophene Polyethylene Oxide Nanofibers Using Electrospinning. *Synth. Met.* **2008**, *158*, 577−584.

(24) Stachewicz, U.; Bailey, R. J.; Wang, W.; Barber, A. H. Size Dependent Mechanical Properties of Electrospun Polymer Fibers From a Composite Structure. *Polymer* **2012**, *53*, 5132−5137.

(25) Nakielski, P.; Pawłowska, S.; Pierini, F.; Liwińska, W.; Hejduk, P.; Zembrzycki, K.; Zabost, E.; Kowalewski, T. A. Hydrogel Nanofilaments via Core-Shell Electrospinning. *PLoS One* **2015**, *10*, e0129816−e0129832.

(26) Pierini, F.; Lanzi, M.; Nakielski, P.; Pawłowska, S.; Zembrzycki, K.; Kowalewski, T. A. Electrospun Poly(3-hexylthiophene)/Poly-(ethylene oxide) Graphene Oxide Composite Nanofibers: Effects of Graphene Oxide Reduction. *Polym. Adv. Technol.* **2016**, *27*, 1465−1475.

(27) Pierini, F.; Lanzi, M.; Lesci, I. G.; Roveri, N. Comparison Between Inorganic Geomimetic Chrysotile and Multiwalled Carbon Nanotubes in the Preparation of One-Dimensional Conducting Polymer Nanocomposites. *Fibers Polym.* **2015**, *16*, 426−433.

(28) Oosterbaan, W. D.; Bolsee, J.-C.; Gadisa, A.; Vrindts, V.; Bertho, S.; D'Haen, J.; Cleij, T. J.; Lutsen, L.; McNeill, C. R.; Thomsen, L.; Manca, J. V.; Vanderzande, D. Alkyl-Chain-Length-Independent Hole Mobility via Morphological Control with Poly(3-alkylthiophene) Nanofibers. *Adv. Funct. Mater.* **2010**, *20*, 792−802.

(29) Babel, A.; Li, D.; Xia, Y.; Jenekhe, S. A. Electrospun Nanofibers of Blends of Conjugated Polymers: Morphology, Optical Properties, and Field-Effect Transistors. *Macromolecules* **2005**, *38*, 4705−4711.

(30) Lanzi, M.; Salatelli, E.; Di-Nicola, F. P.; Zuppiroli, L.; Pierini, F. A New Photocrosslinkable Oligothiophene for Organic Solar Cells with Enhanced Stability. *Mater. Chem. Phys.* **2017**, *186*, 98−107.

(31) Bedford, N. M.; Dickerson, M. B.; Drummy, L. F.; Koerner, H.; Singh, K. M.; Vasudev, M. C.; Durstock, M. F.; Naik, R. R.; Steckl, A. J. Nanofiber-Based Bulk-Heterojunction Organic Solar Cells Using Coaxial Electrospinning. *Adv. Energy Mater.* **2012**, *2*, 1136−1144.

(32) Camposeo, A.; Greenfeld, I.; Tantussi, F.; Pagliara, S.; Moffa, M.; Fuso, F.; Allegrini, M.; Zussman, E.; Pisignano, D. Local Mechanical Properties of Electrospun Fibers Correlate to Their Internal Nanostructure. *Nano Lett.* **2013**, *13*, 5056−5062.

(33) Dante, M.; Yang, C.; Walker, B.; Wudl, F.; Nguyen, T. Q. Self-Assembly and Charge-Transport Properties of a Polythiophene−Fullerene Triblock Copolymer. *Adv. Mater.* **2010**, *22*, 1835−1839.

(34) Miyanishi, S.; Zhang, Y.; Hashimoto, K.; Tajima, K. Controlled Synthesis of Fullerene-Attached Poly(3-alkylthiophene)-Based Copolymers for Rational Morphological Design in Polymer Photovoltaic Devices. *Macromolecules* **2012**, *45*, 6424−6437.

(35) Chi, D.; Qu, S.; Wang, Z.; Wang, J. High Efficiency P3HT:PCBM Solar Cells with an Inserted PCBM Layer. *J. Mater. Chem. C* **2014**, *2*, 4383−4387.

DOI: 10.1021/acs.macromol.7b00857
Macromolecules 2017, 50, 4972−4981

(36) Vandewal, K.; Tvingstedt, K.; Gadisa, A.; Inganäs, O.; Manca, J. V. On the Origin of the Open-Circuit Voltage of Polymer-Fullerene Solar Cells. *Nat. Mater.* **2009**, *8*, 904−909.
(37) Yang, Y.; Chen, W.; Dou, L.; Chang, W.-H.; Duan, H.-S.; Bob, B.; Li, G.; Yang, Y. High-Performance Multiple-Donor Bulk Heterojunction Solar Cells. *Nat. Photonics* **2015**, *9*, 190−198.
(38) Yu, X.; Yang, H.; Wu, S.; Geng, Y.; Han, Y. Microphase Separation and Crystallization of All-Conjugated Phenylene-Thiophene Diblock Copolymers. *Macromolecules* **2012**, *45*, 266−274.
(39) Stalmach, U.; de Boer, B.; Videlot, C.; van Hutten, P. F.; Hadziioannou, G. Semiconducting Diblock Copolymers Synthesized by Means of Controlled Radical Polymerization Techniques. *J. Am. Chem. Soc.* **2000**, *122*, 5464−5472.
(40) Guo, X.; Zhou, N.; Lou, S. J.; Smith, J.; Tice, D. B.; Hennek, J. W.; Ponce Ortiz, R.; Lopez Navarrete, J. T.; Li, S.; Strzalka, J.; Chen, L. X.; Chang, R. P. H.; Facchetti, A.; Marks, T. J. Polymer Solar Cells with Enhanced Fill Factors. *Nat. Photonics* **2013**, *7*, 825−833.

DOI: 10.1021/acs.macromol.7b00857
Macromolecules 2017, 50, 4972−4981